



Improved uniformity in cylindrical cup wall thickness at elevated temperatures using deep drawing process for SPCC sheet steel

The-Thanh Luyen¹ · Duc-Toan Nguyen²

Received: 14 September 2022 / Accepted: 23 May 2023 / Published online: 6 June 2023
© The Author(s), under exclusive licence to The Brazilian Society of Mechanical Sciences and Engineering 2023

Abstract

This study aimed to investigate the effect of elevated temperatures, combined with the blank holder force and punch radius, on the thickness distribution of cylindrical cups in the deep drawing of SPCC sheet steel. Numerical simulations and corresponding experiments were conducted to evaluate the performance of the hardening equation that combines anisotropy coefficient based on Hill's 48 stress models in simulating and comparing the deformed cylindrical cup shapes at room and elevated temperatures. The results showed good agreement between simulation and experimental data and confirmed that the thinness of the cylindrical cup increased at elevated temperatures due to the indeterminacy of the blank holder force parameter. To improve the thickness uniformity of the cylindrical cups, the Taguchi analysis design and ANOVA variance were employed to optimize the blank holder force, punch radius, and elevated temperature parameters. The optimal parameters were selected for simulation and experiment to confirm the uniformity of the cup thickness, with a thickness deviation of only 1.62% between simulation and experiment. This study provides valuable insights into the process parameters and conditions necessary for the deep drawing of cylindrical cups with uniform thickness distribution.

Keywords Thickness distribution · Deep drawing at elevated temperatures · SPCC sheet steel · FEM · Taguchi method

1 Introduction

Sheet-forming technology plays an essential role in the aerospace, automotive, and shipbuilding industries. In particular, the deep drawing process is normally used to manufacture cup or box-shaped parts with large forming heights. In the deep drawing process, numerous studies on the influence of parameters such as the blank holder force (BHF), punch/die corner radius, and drawing ratios on the formability of cylindrical cups have been conducted to limit the phenomenon of wrinkles on the cup rim and the uniform thinness of the

cylindrical cup. The uniformity of the cylindrical cup wall is essential for the long-term working ability of products, leading to the design of suitable molds. Kim and Lee [1] studied the effect of ultrasonic vibration on the deep drawing process of cylindrical cups from cold-rolled carbon (SPCC) steel sheets through experiments and simulations. The results showed that the forming force tended to decrease when ultrasonic vibration was applied. Wahyanti et al. [2] studied the effect of friction on the phenomenon of wrinkles and thinning during deep drawing on two materials, SCGA and SPCC, and concluded that the higher the friction coefficient, the higher the degree of thinning/wrinkling on the cylindrical cup. Jankree et al. [3] studied the influence of defects at the rim while deep drawing the SPCC cylindrical cup using two different types of dies, such as conventional and variable multi-draw radius (MDR) dies. Research has shown that the defects at the cup rim are improved when using a variable-radius die. Phanitwong [4] studied the increase in formability when using MDR dies for SPCC cold-rolled steel sheets and confirmed that using an MDR mold improves the formability and rim defects of SPCC cylindrical cups.

The finite element method (FEM) is commonly used when investigating sheet metal forming because it provides

Technical Editor: Izabel Fernanda Machado.

✉ Duc-Toan Nguyen
toan.nguyenduc@hust.edu.vn

The-Thanh Luyen
luyenthethanh@gmail.com

¹ Faculty of Mechanical Engineering, Hungyen University of Technology and Education, Hungyen 160000, Vietnam

² School of Mechanical Engineering, Hanoi University of Science and Technology, 1A-Dai Co Viet Street, Hai Ba Trung District, Hanoi City 100000, Vietnam

useful results on stress and strain in general applications. Several studies have been conducted on the effects of geometrical and technological parameters on cylindrical cup thickness [5–9]. Recent simulated studies have focused on the effect of mesh element type [10], anisotropy [11], punch–die misalignment [12], BHF [13], and friction coefficient [14] on the distribution of cup wall thickness in deep drawing processes. Jawad et al. [15] used FE simulation and corresponding experiments to investigate the influence of punch radii on the thinness of cylindrical cups when forming low-carbon steel with a sheet thickness of 0.7 mm. Walzer and Liewald [16] studied the FE simulation of the deep drawing processes for cylindrical cups in two cases, with and without using the embossing technique. The embossing technique can significantly affect the thinning and redistribution of thickness to other locations on the cylindrical cup. Zhang et al. [17] studied the BHF distribution for the deep drawing process using a blank holder divided into double rings and concluded that wrinkles on the cylindrical cup could be better eliminated with appropriate parameter selection. Salahshoor et al. [18] examined the effect of several die/punch geometry parameters to improve the formability of a cylindrical cup in hydrodynamic deep drawing assisted by radial pressure and showed that increasing the peak pressure causes a partial reduction in thinning in important areas. The thinness of the part and the maximum force were reduced by reducing the friction between the blank/blank holder. In addition, increasing the coefficient of friction between the punch/blank to 0.2 will improve the formability and decrease the thinness of the part. A clear description of the anisotropy of plastic deformation is required for the numerical simulation of sheet-metal forming processes. For isotropic metallic materials, the von Mises stress function [19] is often used to describe stress. However, this is not true for anisotropic materials, particularly sheet metals. The von Mises stress function can be modified by introducing additional parameters to evaluate anisotropy. These parameters can be adjusted according to the set of experimental data obtained by subjecting the material under consideration to mechanical testing. Hill's quadratic stress function (Hill'48 [20] and Hill'52 [21]) is the most frequently used stress function of this type. The anisotropic stress criteria were studied by Banabic et al. [22]. Recently, experimental methods for identifying the anisotropic patterns and advanced criteria for anisotropic polycrystalline materials with different crystal structures have been proposed. Yong et al. [23] compared the accuracy of Hill'48 [20], Barlat89 [24], and Yld2000 [25] stress models in the springback simulation of U-shaped parts made from MP980 material. The results showed that the Yld2000 stress model with eight parameters markedly improved the prediction accuracy of the springback of the U-shaped part. Chen et al. [26] used the cyclic loading kinematic hardening model based on the Hill'48 anisotropy

criterion and concluded that this combination will provide accurate predictions in the numerical simulation of the reverse deep drawing process. Zein et al. [5] predicted the springback and thickness/thinness distributions of a cylindrical cup using FEM simulation. The technological, geometrical, and physical parameters were changed during the deep drawing process. The study recommended specific values for the technological and geometrical parameters to reduce the thinness and springback of a cylindrical cup. Padmanabhana et al. [27] studied and optimized the deep drawing process of cylindrical cups made from stainless steel. The FEM was combined with Taguchi orthogonal arrays and analysis of variance (ANOVA) to optimize three input parameters, such as the radius of the die corner, BHF, and friction coefficient, which affect the uniformity of the cup thickness after deep drawing in this study. The bottom of the cup was thinned, and the top and rim of the cup were thickened. Raju et al. [28] studied the effect of BHF and the die/punch corner radius on the thickness distribution of cylinder cups when deep drawing an AA6061 aluminum alloy sheet of 0.8 mm thickness. This study used Taguchi orthogonal arrays and ANOVA analysis of variance to optimize the input parameters. The results show that the die corner radius has a significant influence (66.49%), followed by the BHF (29.16%) and the (R_p) punch corner radius (9.23%).

Very few studies have evaluated the effect of heating temperature on the uniform thinness of the cylindrical cup wall in combination with the BHF and punch/die geometric parameters. Thermal assistance during plastic deformation typically improves the formability of sheet metals. However, if the BHF is not appropriately selected during deep drawing processing at elevated temperatures, it will affect the uniformity of the cup wall and increase the possibility of thinness at critical positions. Therefore, this study aimed to determine a reasonable set of parameters for deep drawing cylindrical cups at warm temperatures to ensure uniformity of the cup wall through the Taguchi experimental algorithm and ANOVA variance analysis. Investigations of the BHF on cup wall thinness were carried out to determine the preliminary BHF region by numerical simulation. The corresponding experiments were compared with the simulation results to confirm good agreement through deviation errors. The effect of the warm temperature on the cup wall thinness/uniformity was then investigated using a FEM simulation. The simulation results and corresponding experiments showed that the thinness at critical positions at elevated temperatures was higher than that at room temperature with the same BHF. Therefore, the Taguchi method combined with ANOVA has been shown to be effective for selecting the appropriate parameter values and optimizing cup wall thinness. Simulation results with the appropriate parameters set for BHF = 8 KN, R_p = 8 mm, and T = 250 °C to improve the cup wall thickness and thinness uniformity. The verification experiment with the most significant deviation of 1.62%

in the cup wall thickness showed a good agreement with the simulation results.

2 Material properties

2.1 Chemical composition of SPCC sheet steel

In this study, tests were performed on SPCC sheet steel to obtain the necessary data to develop a model that predicts the formability of the cylindrical cup deep stamping process. The chemical composition of the materials is listed in Table 1.

2.2 Determining the mechanical properties of experimental materials

The mechanical properties of the SPCC sheet steel were determined using uniaxial tensile tests. The tensile tests were conducted at room temperature and high temperatures of 150 °C and 250 °C. The measurement results are shown in Fig. 1, and the material properties are listed in Table 2. This study used the Kim–Tuan model [29] corresponding to Eq. (1) to describe the results. The properties of the SPCC sheet material are shown in Fig. 1.

$$\text{Kim - Tuan : } \bar{\sigma} = \sigma_0 + K(1 - \exp(-t\bar{\epsilon}))(\bar{\epsilon} + 0.002)^h \tag{1}$$

where: $\bar{\sigma}$, and $\bar{\epsilon}$ represent true stress and true strain, respectively. The hardening parameters, namely σ_0 ; K ; t ; and h , are listed in Table 2

3 FE simulation and experimental results of deep drawing process

3.1 Experimental setup

The experimental products were cylindrical cups made of an SPCC sheet steel with a thickness of 0.6 mm. This study aimed to determine the thinning of cylindrical cups using both simulations and experiments. The geometrical parameters of the die/punch set are shown in Fig. 2a with a punch diameter (d_p) of 67 mm, die corner radius (R_d) of 6 mm, clearance between the punch and die (W_c) of 1 mm, and a varied punch corner radius (R_p) of 6 to 8 mm. The experimental die/punch/blank-holder setup is shown in Fig. 2b. The BHF and temperature (T) in the deep drawing process were studied with variable values of BHF from 6 to 10 kN and temperature T from 25 to 250 °C. The deep drawing process of the SPCC cold-rolled steel

Table 1 Chemical composition of SPCC sheet steel

Material	C	Mn	P	S
SPCC	<0.1	<0.45	<0.035	<0.04

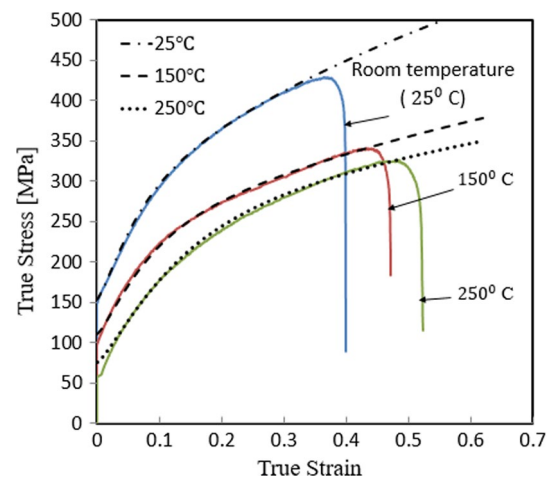


Fig. 1 Flow stress curves of SPCC sheet steel at different temperatures

sheets for a cylindrical cup was performed on a dual-dynamic hydraulic press with a load capacity of 150 tons. The oil used in the deep drawing process is commercially available.

The thickness of the cylindrical cup part after deformation was measured using an Axiovert 40 MAT microscope and analyzed in the micrometer-sized region. Cylindrical cups were cut, machined, and tested for their thickness at eight positions. As shown in Fig. 3, the curvature radius of the cylindrical cup at position 5 was magnified to a micrometer size of 500 μm.

3.2 FE simulations of deep drawing process

In this study, the cylindrical cup deep drawing process was simulated using ABAQUS 6.13 software [30]. Figure 4 depicts the FE simulation 3D model for the deep drawing process, in which the punch is fixed and the blank-holder and die are moved longitudinally to achieve the forming

Table 2 Properties of SPCC sheet steel at different temperatures

Materials	SPCC		
	Room temperature	150 °C	250 °C
Yield stress (MPa)	152.1	110.6	72.5
Tensile strength (MPa)	428.8	341.8	326.3
Elastic modulus (E , kN/mm ²)	210	171	163
K (MPa)	460	326.3	324.6
t	25.86	20.16	12.02
h	0.48	0.42	0.35
Density (ρ kg/mm ³)	7.8e−06		
Elastic modulus (E , kN/mm ²)	210		
Poisson ratio (μ)	0.3		

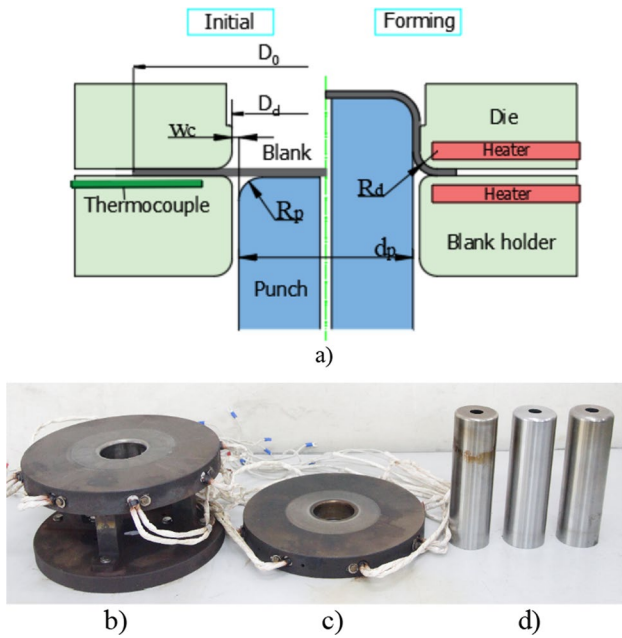


Fig. 2 Experimental system for the deep drawing process: **a** The geometry dimensions; **b** Die; **c** Blank holder and **d** Punch

cup depth through the deformation state. The rigid body model was used to analyze the punch, blank holder, and die, whose displacements were activated by reference points. The blank workpiece was modeled using deformed and reduced integrated shell modeling (S4R). In this study, the friction between the punch, die, and blank holder during deep drawing was obtained from [6, 31].

The anisotropic state of the material and the elastic and plastic deformation of the SPCC sheet steel were simulated based on the stress criteria of Hill'48.

Specifically, the equivalent stress determined by the Hill stress function 1948 [20] is calculated as follows:

$$\bar{\sigma} = \sqrt{G\sigma_1^2 + F\sigma_2^2 + H(\sigma_1 - \sigma_2)^2}. \tag{2}$$

Fig. 3 Measured thickness of cylindrical cups after the deep drawing process

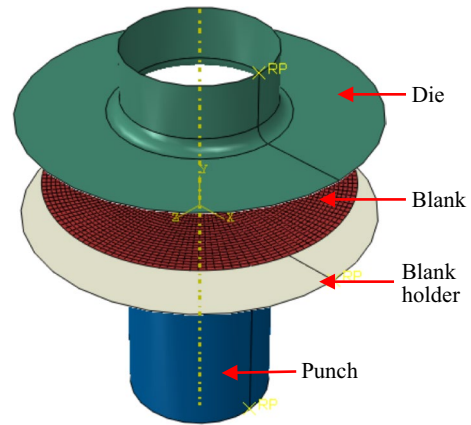
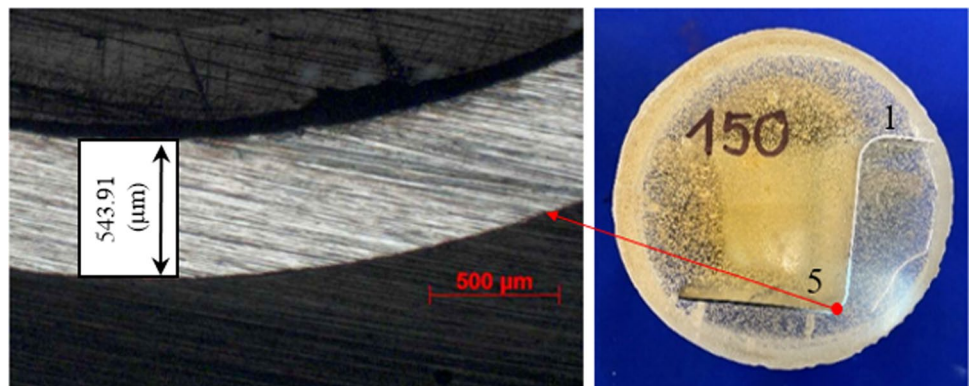


Fig. 4 FE model deep drawing in Abaqus

where: σ_1 and σ_2 represent the normal Cauchy stresses. The values of G , F , and H are constants that can be calculated based on the given value of R , as follows:

$$\begin{cases} F = \frac{1}{2R_{22}^2} + \frac{1}{2R_{33}^2} - \frac{1}{2R_{11}^2} \\ G = \frac{1}{2R_{11}^2} + \frac{1}{2R_{33}^2} - \frac{1}{2R_{22}^2} \\ H = \frac{1}{2R_{11}^2} + \frac{1}{2R_{22}^2} - \frac{1}{2R_{33}^2} \end{cases} \tag{3}$$

$$\begin{cases} R_{22} = \sqrt{\frac{r_{90}(r_0 + 1)}{r_0(r_{90} + 1)}} \\ R_{33} = \sqrt{\frac{r_{90}(r_{90} + 1)}{(r_0 + r_{90})}} \end{cases} \tag{4}$$

where: the anisotropy ratio is measured at 0° and 90° loading angles with respect to the rolling direction of the parent sheet, denoted by r_0 and r_{90} , respectively. Anisotropy ratios are represented by R_{11} , R_{22} , R_{33} , R_{12} , R_{13} and R_{23} .

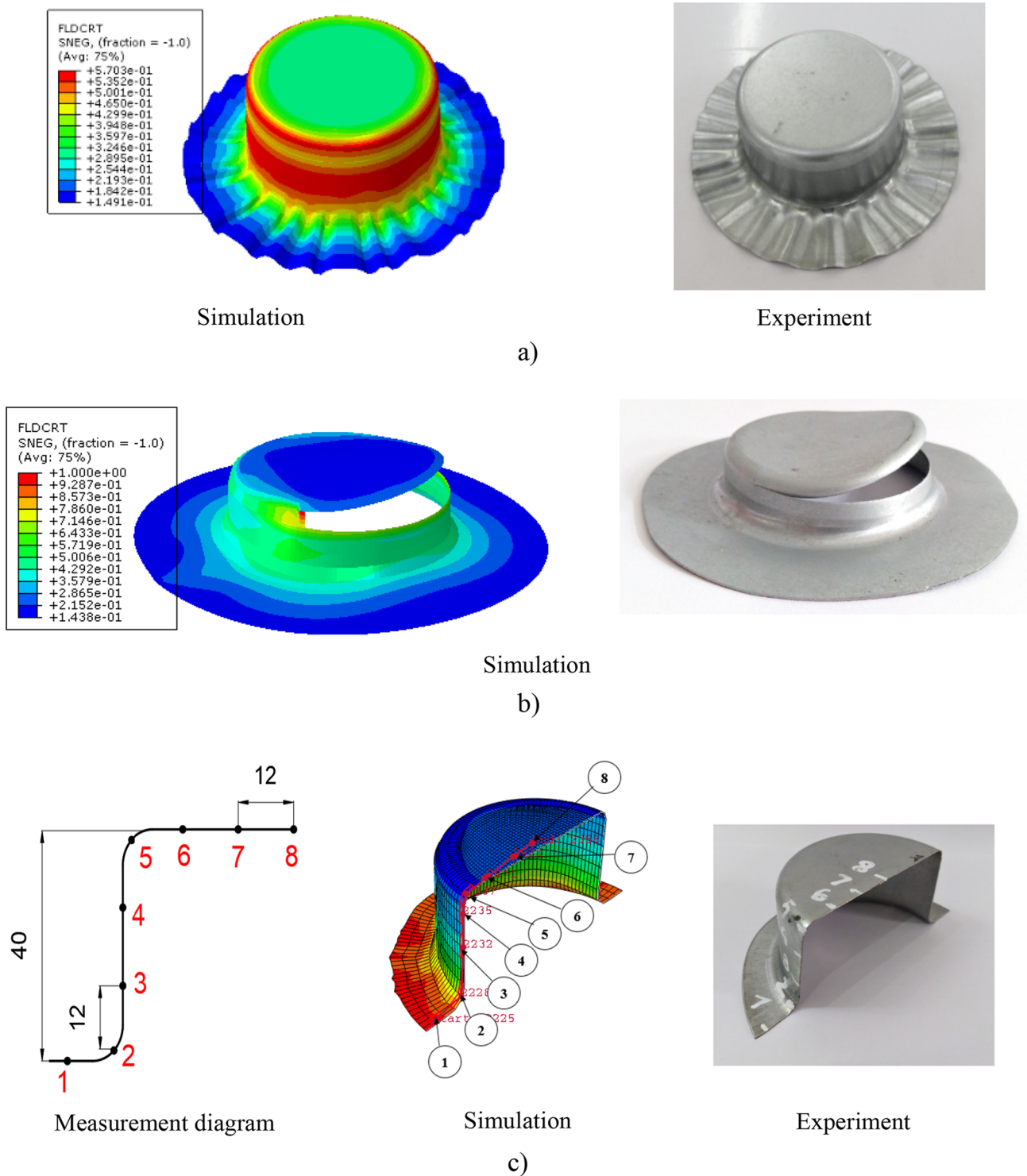


Fig. 5 Deformed shapes of cylindrical cups **a** Wrinkle occurrence for a BHF of 5 kN; **b** Fracture occurrence for a BHF of 18 kN, **c** Thickness determination and **d** Thickness distribution

For the plane stress case, only four stress ratios are required. Here, assuming that the rolling direction (RD) is the user-defined reference stress, $R_{11}=1$; further, R_{22} and R_{33} are calculated according to the system of Eqs. (4) as 1.0143

and 1.2026, respectively. This anisotropy ratio value was declared in the material model to investigate the fracture occurrence through FE simulation.

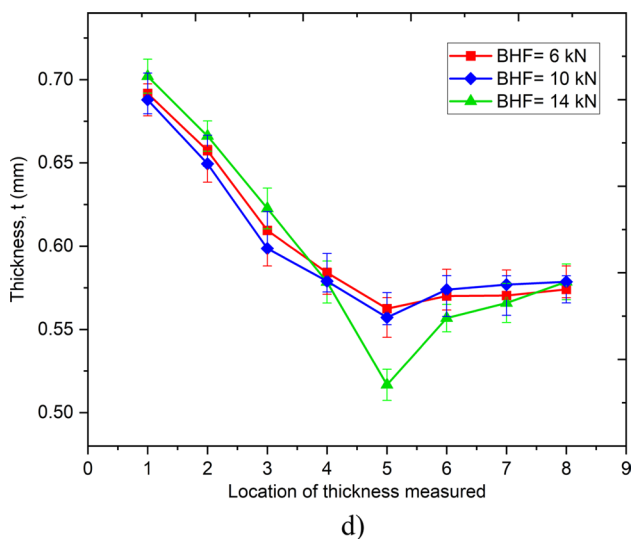


Fig. 5 (continued)

4 Results and discussion

4.1 The limitation range of blank holder force (BHF)

To investigate the effect of the BHF on the uniformity of the thickness of the cylindrical cup, simulations and corresponding experiments were carried out using a workpiece diameter of 140 mm (D0) and a fixed deep drawing depth of 40 mm (H). The BHF of the deep drawing process was then selected, starting from the lower limit region when the part was wrinkled on the rim. When the BHF was less than 6 kN, the cylindrical cup appeared wrinkled, as shown in Figure 5a. As the BHF increased, the wrinkling tended to decrease. However, the cylindrical cup's formability was limited by the deformation of the side wall of the cylindrical cup. If the strain of the cylindrical cup reaches the maximum value, a fracture will occur at the punch corner, as shown in Figure 5b, with a BHF of 18 kN. Thus, the BHF was varied from 6 to 14 kN to investigate the cylinder thickness distribution based on both the numerical simulations and corresponding experiments. Figure 5c shows the measurements of eight points on the cross-section of the cylinder cup profile. Figure 5d shows that the cylindrical cup thickness suddenly decreased at point 5 in the case of 14 kN of BHF. Therefore, this study is limited to the BHF range from 6 to 10 kN.

4.2 The deviation between FE simulation and experiment on thickness distribution at room temperature

To evaluate the difference between the simulation and experimental results, cup thickness was measured after deep drawing at room temperature with a BHF of 10 kN (Fig. 6 (a)).

The measurement results are shown in Fig. 6b and Table 3, with a deviation error ($\Delta t(\%)$) calculated using Eq. (5). The measurement results show that the rim of the cup tends to thicken (from positions 1–3), while the measuring positions from positions 4 to 8 of the cylindrical cup were thinner than the average thickness of the sheet. Table 3 and Fig. 6b show that, the average thickness distribution in the FE simulation is close to the average thickness obtained from the respective experimental results. The difference in the cylindrical cup thickness between the thinnest point and average thickness ($\Delta t_{\max}(\%)$) was calculated using Eq. (6). The thickness at the thinnest measurement position in the simulation model was 7.17% thinner than the average thickness. Meanwhile, on experimental results, the thinnest measuring position was 8.13% thinner than the average thickness. The comparison results showed good agreement between the FE model and the corresponding experiments in measuring the thickness distribution.

$$\Delta t(\%) = \frac{|t_S - t_E|}{t_E} \cdot 100\% \quad (5)$$

$$\Delta t_{\max}(\%) = \frac{|t_{\min} - t_A|}{t_A} \cdot 100\% \quad (6)$$

where t_S , t_E , t_{\min} , and t_A are the simulation, experimental, minimum, and average cup thicknesses, respectively.

4.3 Thickness distribution of cylindrical cups at elevated temperatures

To investigate the effect of heat treatment on the thickness distribution when deep drawing SPCC metal sheets, simulations and corresponding experiments were performed, as shown in Fig. 7a. The results of measuring the thickness of the cylindrical cup at 150 °C and 250 °C are shown in Table 4 and Fig. 7b. The obtained results showed that the thickness on the cup rim had the highest value (position 1) and tended to become thinner at the die corner radius (position 2), and then at the cup wall (positions 3 and 4); finally, the thinnest value was observed at the punch corner radius (position 5) in both the simulation and experiment.

At the cup rim measurement point (position 1), the sheet metal was the thickest, and at the punch radius measurement point (position 5), it had the thinnest value (Fig. 7c). The deviation error between the simulation and experiment was determined using Eq. (5). The most significant deviation values at measuring position 1 are 2.67% and 3.14% at 150 and 250 °C, respectively. Meanwhile, the smallest deviations at the elevated temperatures of 150 and 250 °C were 0.68% (position 8) and 0.29% (position 7), respectively. The difference in the cylindrical cup thickness between the thinnest point and average thickness was calculated using Eq. (6).

Fig. 6 Deformed cup **a** and thickness distribution of the cylindrical cup vs deviation error between FE simulation and experiment **b** at room temperature

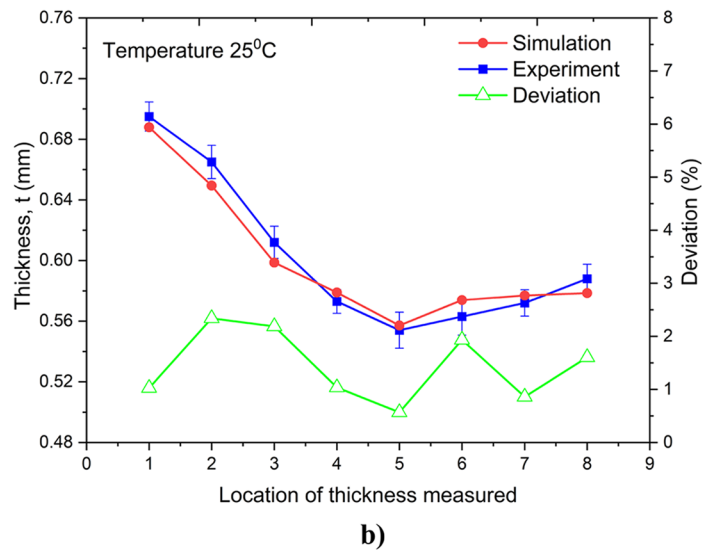
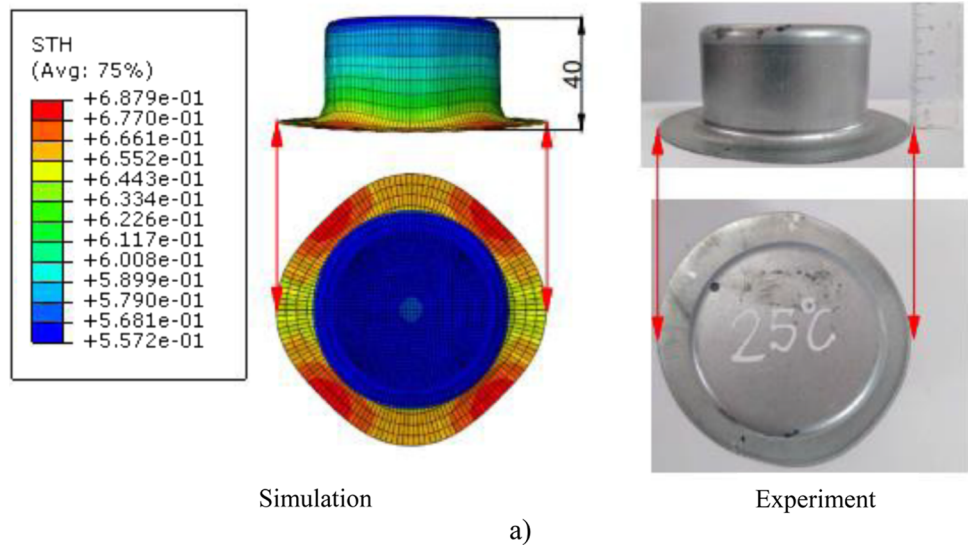


Table 3 Deviation between FE simulation and experiment on cylindrical cup thickness at room temperature

Measured thickness (mm) at locations	Experiment	Simulation	% Δt deviation
1	0.695	0.688	1.02
2	0.665	0.649	2.34
3	0.612	0.599	2.19
4	0.573	0.579	1.04
5	0.554	0.557	0.57
6	0.563	0.574	1.93
7	0.572	0.577	0.86
8	0.588	0.579	1.60
Average	0.603	0.600	0.43

The thicknesses at the thinnest measurement positions in the simulation were less than 8.14% and 8.47% compared to the average thickness values at 150 and 250 °C, respectively. Meanwhile, the thinnest measuring positions compared to the average thickness value in the corresponding experiments were 9.48% and 10.26% thinner at 150 and 250 °C, respectively.

At the cup rim measurement point (position 1) the sheet metal tends to the thickness and at the punch radius measurement point (position 5) gives the thinnest value (Fig. 8). Deviation error between simulation and experiment is determined according to Eq. (5). The largest deviation values at measuring position no 1 are 2.67% and 3.14% for 150 and 250 °C, respectively. Meanwhile, the smallest deviations with the elevated temperature of 150 and 250 °C are 0.68% (position 8) and 0.29% (position 7), respectively. The difference in cylindrical cup thickness between the thinnest

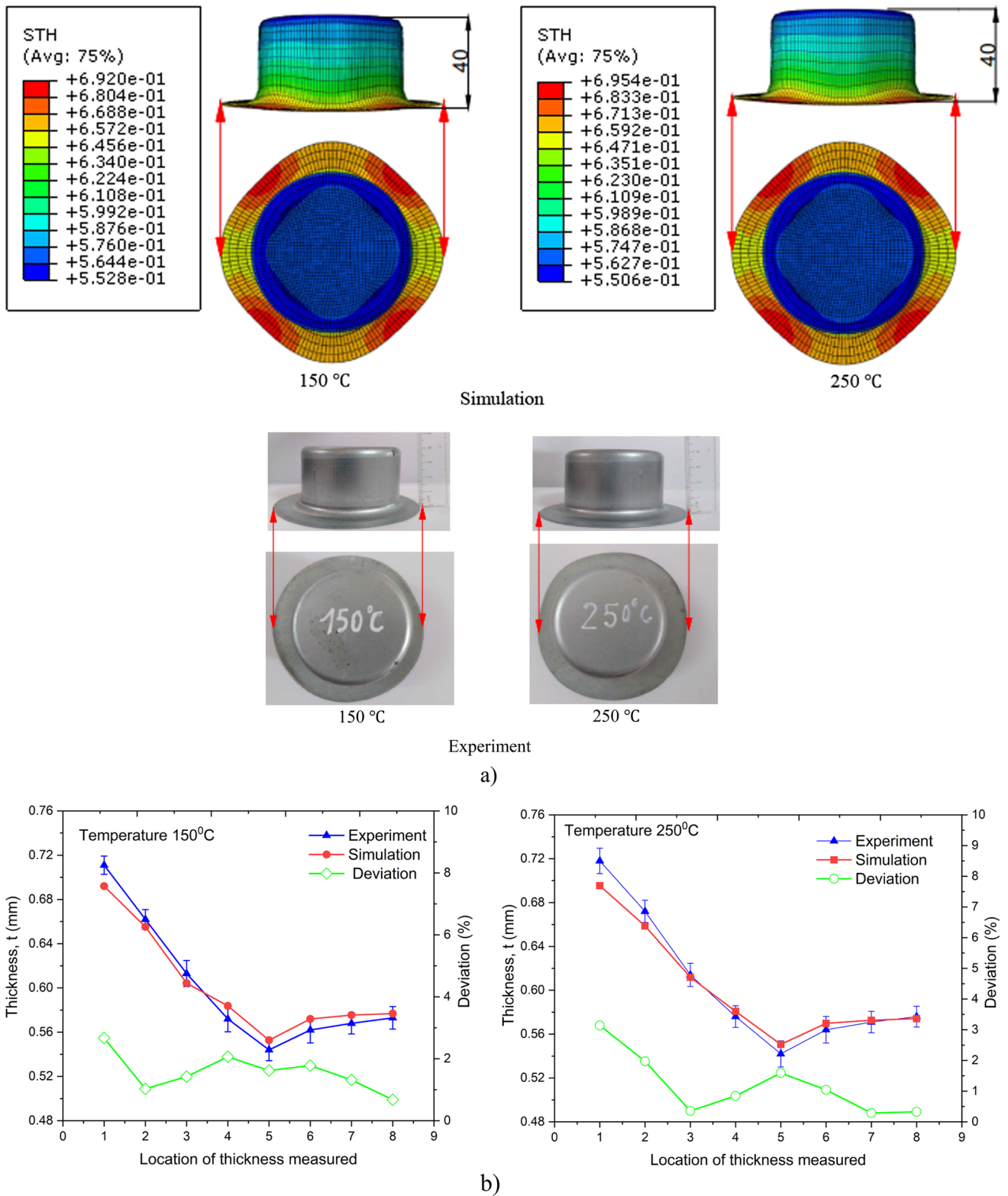


Fig. 7 Deformed cups: **a** thickness distribution of the cylindrical cup with a deviation error between FE simulation and experiment and **b** measured thickness at thickest/thinnest positions **c** at elevated temperatures

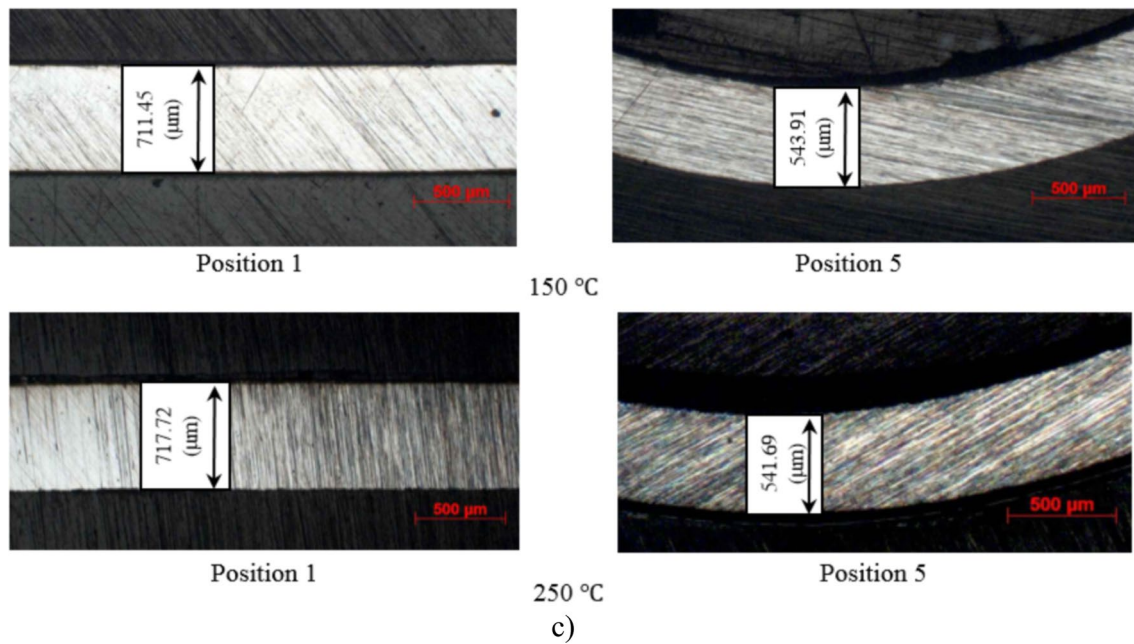


Fig. 7 (continued)

Table 4 Deviation between FE simulation and experiment on cylindrical cup thickness at elevated temperature

Measured thickness (mm) at locations	150 °C			250 °C		
	Experiment	Simulation	Deviation % Δt	Experiment	Simulation	Deviation % Δt
1	0.711	0.692	2.67	0.718	0.695	3.14
2	0.662	0.655	1.03	0.672	0.659	1.97
3	0.613	0.604	1.42	0.614	0.612	0.36
4	0.572	0.584	2.06	0.576	0.581	0.84
5	0.544	0.553	1.62	0.542	0.551	1.59
6	0.562	0.572	1.78	0.564	0.570	1.04
7	0.568	0.575	1.32	0.571	0.573	0.29
8	0.573	0.577	0.68	0.576	0.574	0.33
Average	0.601	0.602	0.15	0.604	0.602	0.39

point and the average thickness is calculated by Eq. (6). The thicknesses at the thinnest measurement positions on the simulation are thinner than 8.14% and 8.47% compared to the average thickness value at 150 and 250 °C, respectively. Meanwhile, the thinnest measuring positions compared to the average thickness value in the corresponding experiments are 9.48% and 10.26% thinner at 150 and 250 °C, respectively.

4.4 Input parameter optimization on the thickness distribution of cylindrical cups

The analysis of the thickness distribution of the cylindrical cups at room and elevated temperatures shows that

the thickness at the thinnest measuring position tends to decrease with increasing heating temperature. This is in contrast to previous studies [29, 32] on the effect of increasing temperature on the uniform thickness distribution and thinness at critical positions. This phenomenon can be explained by the BHF value being kept constant during deep drawing at room and high temperatures. In particular, a high temperature can improve the formability of the SPCC material but is limited by the selected BHF value. Therefore, it is necessary to examine the relationship between the parameters, such as the BHF, punch radius (R_p), temperature (T), and the uniform thickness distribution (t) of the cylindrical cup. The effects of BHF, R_p , and T on the uniformity of the cylindrical cup thickness can be predicted, analyzed,

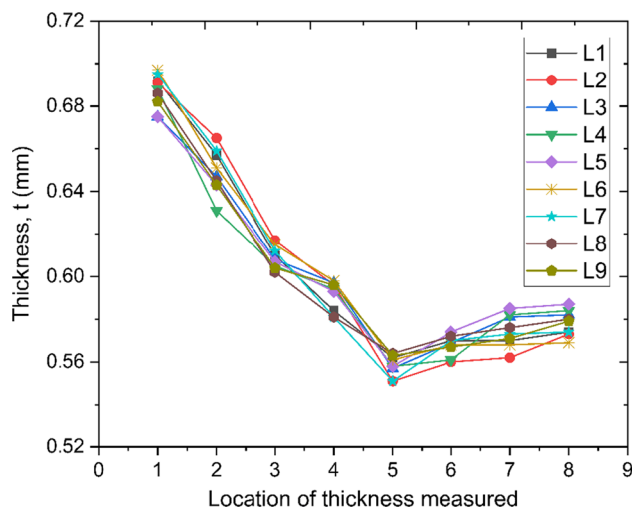


Fig. 8 Thickness distribution of sheet metal from FEM simulation

Table 5 Input parameters and their levels

Parameters		levels		
		1	2	3
Blank holder force (BHF)	KN	6	8	10
Punch radius (R_p)	mm	4	6	8
Temperatures (T)	°C	25	150	250

Table 6 Taguchi L9 orthogonal array

No.	BHF (KN)	R_p (mm)	T (°C)
1	6	4	25
2	6	6	150
3	6	8	250
4	8	4	150
5	8	6	250
6	8	8	25
7	10	4	250
8	10	6	25
9	10	8	150

and evaluated using simulation data. The selected optimal parameters of BHF, R_p , and T were tested through corresponding experiments. During the simulations, 3 levels of each input parameter were selected (Table 5). Therefore, the orthogonal array L9 was used to design the experimental design. A minimum of nine experiments were needed to check the effect of the variable parameters during the simulation. Using the Taguchi orthogonal algorithm, the number of experimental designs were reduced from 27 to 9. The simulation results for the sheet metal thickness values

for the selected cases using the Taguchi method are listed in Tables 6 and 7.

The results for the thickness (t) of the nine simulated samples are presented in Table 7 and Fig. 8. The S/N ratios for each experiment are presented in Table 8. The S/N ratio with the characteristic for the thickness of the cylindrical cup is nominal-the-best determined by Eqs. (7) and (8).

$$S/N = -10 \log(\text{MSD}) \tag{7}$$

With the nominal-the-best quality characteristic, MSD is defined as:

$$\text{MSD} = \frac{\bar{y}^2}{S_y^2} \tag{8}$$

where: $\bar{y} = \frac{\sum_{i=1}^r y_i}{r}$, $S_y^2 = \frac{\sum_{i=1}^r (y_i - \bar{y})^2}{r-1}$

Here, y_i are the measured value in the experiment, r is the number of measurements in each experiment, and \bar{y} is the nominal or target value.

The Taguchi method was used for the experimental design in this study to determine the influence of the input parameters on the thickness distribution of cylindrical cups. This method allows each parameter to be evaluated independently and in randomized experiments. The S/N ratio of each control parameter with three levels and their influence on the thickness of the cylindrical cup were analyzed, as shown in Fig. 9. The optimal level of input parameters is the higher value, as shown in Table 9, with the optimal parameters of $M_2N_3P_3$: BHF = 8 KN, R_p = 8 mm, T = 250 °C. The ANOVA results for the cylindrical cup thickness (Table 9) show that the temperature and punch radius have the greatest (38.79%) and smallest (29.01%) influences on the cylindrical cup thickness, respectively.

The deformation results of the cylindrical cup with optimal parameters by simulation and experiment are shown in Fig. 10a and b, respectively. The thickness distribution of the optimal cylindrical cup is presented in Table 10 and Fig. 10c. The deviation between the thinnest point and the average thickness of the optimal cylindrical cup was calculated using Eq. (6). The thickness at the thinnest measurement position in the simulation model was 4.16% thinner than the average measurement value. Meanwhile, the measurement results for the experimental cylindrical cup indicated that the thinnest measuring position was thinner than the average measurement value of 5.78%. The deviation data between the measurement points show that the thinness variation of the optimal cylindrical cup is closest to the average measurement value. The comparison results also show a good agreement in the thickness distribution of cylindrical cups between the FE simulation and the corresponding experiment, with a maximum thickness deviation of 1.62%.

Table 7 The results of measuring the thickness of cylindrical cups in 9 experiments

	Measured thickness (mm) at locations	Taguchi L9								
		L1	L2	L3	L4	L5	L6	L7	L8	L9
1		0.692	0.691	0.675	0.688	0.675	0.697	0.695	0.686	0.682
2		0.657	0.665	0.647	0.631	0.643	0.651	0.659	0.645	0.643
3		0.610	0.617	0.608	0.605	0.607	0.615	0.612	0.602	0.604
4		0.584	0.596	0.597	0.594	0.593	0.598	0.581	0.581	0.596
5		0.562	0.551	0.557	0.558	0.558	0.561	0.551	0.564	0.563
6		0.570	0.560	0.569	0.561	0.574	0.568	0.570	0.572	0.567
7		0.570	0.562	0.581	0.582	0.585	0.568	0.573	0.576	0.571
8		0.574	0.573	0.582	0.584	0.587	0.569	0.574	0.580	0.579
Average		0.602	0.602	0.602	0.600	0.603	0.603	0.602	0.601	0.601

Table 8 S/N ratio

No.	BHF (kN)	R _p (mm)	T (°C)	S/N	$\overline{S/N}$
1	10.0	4	25	22.022	22.571
2	10.0	6	150	21.263	
3	10.0	8	250	23.485	
4	12.5	4	150	23.005	
5	12.5	6	250	23.906	
6	12.5	8	25	21.841	
7	15.0	4	250	21.564	
8	15.0	6	25	22.940	
9	15.0	8	150	23.109	

Table 9 ANOVA results for cylindrical cup thickness

Parameter	S/N ratio			Sum of squares	Contribution percentage(%)
	1	2	3		
BHF (M)	22.257	22.918*	22.538	0.220	30.96
R _p (N)	22.197	22.703	22.812*	0.192	27.01
T (P)	22.268	22.459	22.985*	0.276	38.79
Noise				0.023	3.24
Sum				0.711	100

*)Optimal value

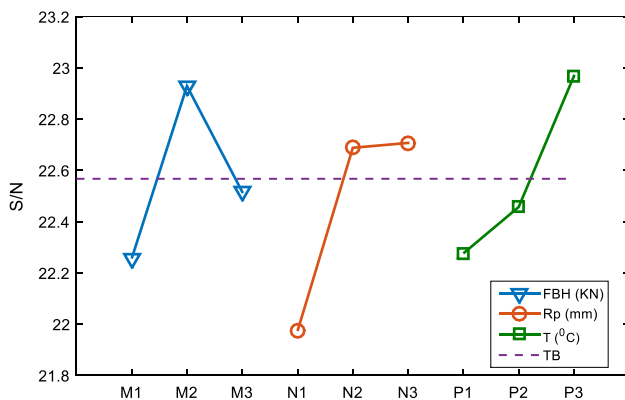


Fig. 9 The S/N ratio varies at different levels

5 Conclusion

The SPCC sheet steel cylinder cups used in this study are being applied in the deep drawing process of fuel filter cups in the automobile industry. This study aims to improve the formability and limit the defects caused by

the thinness of the cup wall. Therefore, FE simulations and corresponding experiments were used to evaluate the influence of room temperature and elevated temperatures in combination with the BHF and punch radius on the thickness distribution of the cylindrical cups of an SPCC sheet steel. The consensus results between the simulation and experiment show the following conclusions:

1. A limited BHF of 6 to 10 kN should be used.
2. The thickness of the cup rim tends to thicken, while the cup wall is thinned and reaches its smallest value at the position of the punch radius.
3. The thinness at the critical positions of cylindrical cups at elevated temperatures will be higher if the BHF value is kept the same at room temperature.
4. To improve the uniformity of the thickness of the cylindrical cups, the optimal parameter set of elevated temperature, punch radius, and BHF should be selected as T = 250 °C, 8 mm, and 8 kN, respectively.
5. In a future work, the obtained results will be used to improve the formability of the deep drawing process with complex and difficult-to-form profiles using local thermal assistance.

Fig. 10 Deformed cylindrical cup after deep drawing process with optimal parameters **a** Simulation; **b** Experiment and **c** thickness distribution

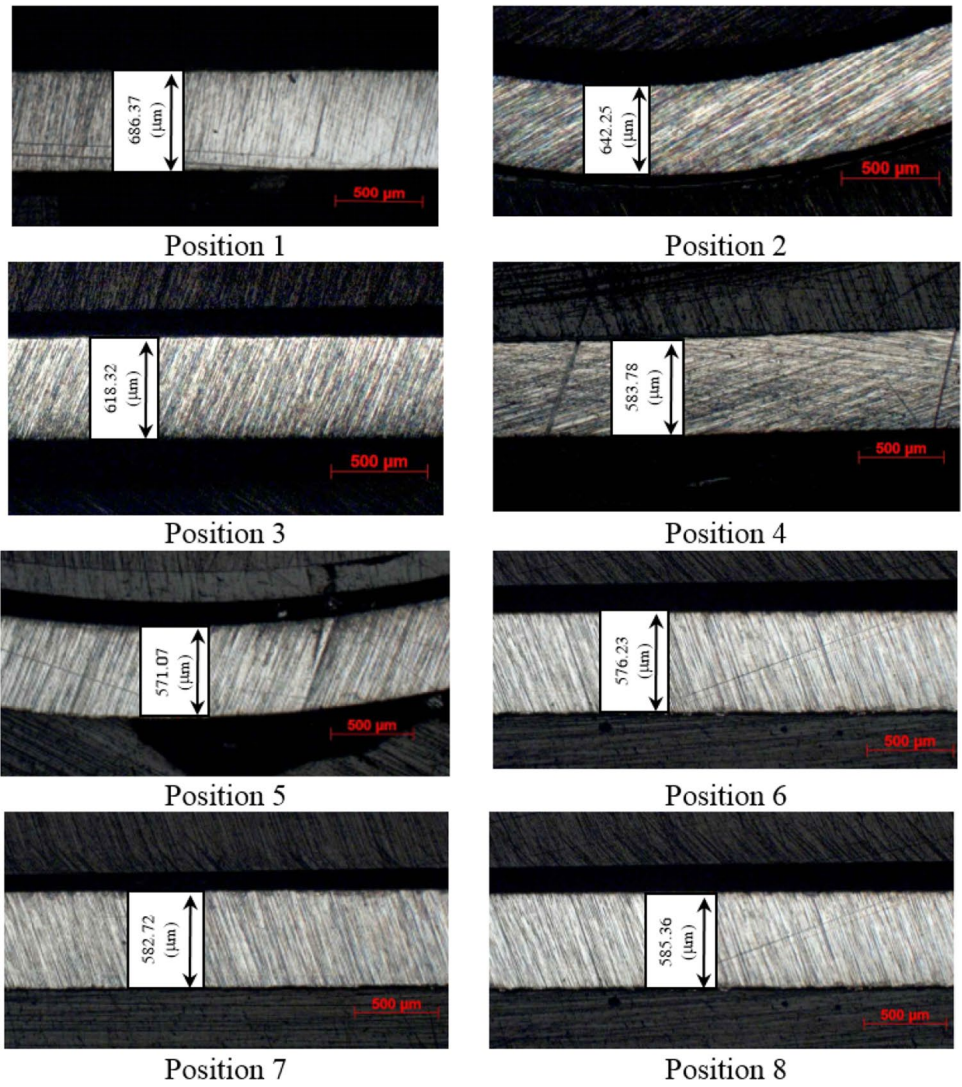
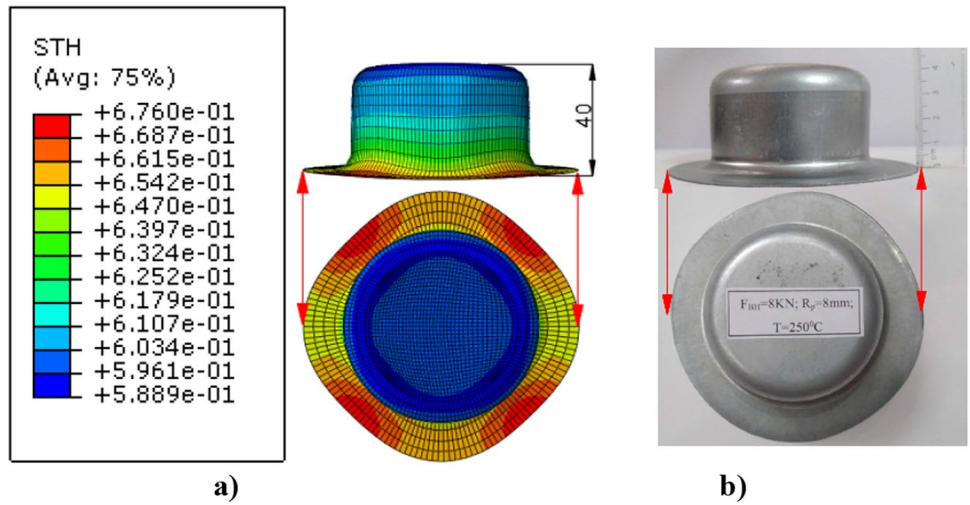
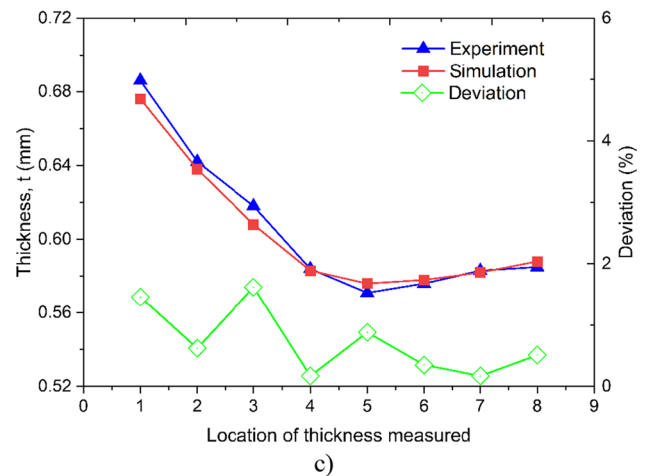


Fig. 10 (continued)

**Table 10** Deviation in thickness distribution of cylindrical cups using optimal parameters between FEM simulation and experiments

Measured thickness (mm) at locations	t (mm)		Deviation % Δt
	Experiment	Simulation	
1	0.686	0.676	1.46
2	0.642	0.638	0.62
3	0.618	0.608	1.62
4	0.584	0.583	0.17
5	0.571	0.576	0.88
6	0.576	0.578	0.35
7	0.583	0.582	0.17
8	0.585	0.588	0.51
Average	0.606	0.601	0.83

Acknowledgements This work was supported by Hanoi University of Science and Technology (HUST) under Grant Number T2022-PC-016.

References

- Kim SW, Lee YS (2014) Investigations on the effect of ultrasonic vibration in cylindrical cup drawing processes. *Key Eng Mater* 622–623:1152–1157. <https://doi.org/10.4028/www.scientific.net/KEM.622-623.1152>
- Wahyanti S, Anggono AD, Siswanto WA (2020) Study of wrinkling and thinning behavior in the stamping process of top outer hatchback part on the SCGA and SPCC materials. *Adv Sci Technol Eng Syst* 5(3):241–248. <https://doi.org/10.25046/aj050331>
- Jankree R, Thipprakmas S (2020) Achievements of nearly zero earing defects on spcc cylindrical drawn cup using multi draw radius die. *Metals (Basel)* 10(9):1–16. <https://doi.org/10.3390/met10091204>
- Phanitwong W, Thipprakmas S (2020) Multi draw radius die design for increases in limiting drawing ratio. *Metals (Basel)* 10(7):1–17. <https://doi.org/10.3390/met10070870>
- Zein H, El Sherbiny M, Abd-Rabou M, El Shazly M (2014) Thinning and spring back prediction of sheet metal in the deep drawing process. *Mater Des* 53:797–808. <https://doi.org/10.1016/j.matdes.2013.07.078>
- The-Thanh L, Tien-Long B, The-Van T, Duc-Toan N (2019) A study on a deep-drawing process with two shaping states for a fuel-filter cup using combined simulation and experiment. *Adv Mech Eng* 11(8):1–11. <https://doi.org/10.1177/1687814019872674>
- Takalkar Atul S, Lenin Babu MC (2019) A review on effect of thinning, wrinkling and spring-back on deep drawing process. *Proc Inst Mech Eng Part B J Eng Manuf* 233(4):1011–1036. <https://doi.org/10.1177/0954405417752509>
- Yang X, Wang B, Zhou J, Dang L, Xiao W, Wang Y (2020) Influence of process parameters on deep drawing of 2060 Al–Li alloy under hot stamping process. *Int J Light Mater Manuf* 3(1):36–42. <https://doi.org/10.1016/j.ijlmm.2019.09.009>
- Luyen T, Tong V, Nguyen D (2021) A simulation and experimental study on the deep drawing process of SPCC sheet using the graphical method. *Alexandria Eng J.* <https://doi.org/10.1016/j.aej.2021.07.009>
- Coër J, Laurent H, Oliveira MC, Manach PY, Menezes LF (2018) Detailed experimental and numerical analysis of a cylindrical cup deep drawing: pros and cons of using solid-shell elements. *Int J Mater Form* 11(3):357–373. <https://doi.org/10.1007/s12289-017-1357-4>
- Bouchaâla K, Ghanameh MF, Essadiqi EH, Faqir M, Meziane M, Mada M (2018) Modeling of anisotropy influence on thickness distribution of deep drawing sheet. In: *ACM International Conference Proceeding Series*, pp 142–146 <https://doi.org/10.1145/3303714.3303737>
- Ghafar AA, Abdullah AB, Mahmood JI (2021) Experimental and numerical prediction on square cup punch–die misalignment during the deep drawing process. *Int J Adv Manuf Technol* 113(1–2):379–388. <https://doi.org/10.1007/s00170-021-06595-5>
- Nezami S, Akbari A, Ahangar S (2017) Parametric investigation of pulsating blank holder's effect in deep drawing process of rectangular Al 1050 Cup. *J Braz Soc Mech Sci Eng* 39:4081–4090. <https://doi.org/10.1007/s40430-017-0845-2>
- Choudhari CS, Khasbage SS (2021) Experimental investigation of forming parameters for square cup deep drawing process. *Mater Today Proc* 44:4261–4267. <https://doi.org/10.1016/j.matpr.2020.10.543>
- Jawad W, Jaafar A (2018) The influence of punch profile radius on deep drawing process in case of a low carbon steel cylindrical cup. *Eng Technol J* 36(10A):1048–1058. <https://doi.org/10.30684/etj.36.10A.5>
- Walzer S, Liewald M (2020) Novel approach to decrease sheet thinning during sheet metal forming by using embossing

- technique. *Proced Manuf* 50(2019):795–799. <https://doi.org/10.1016/j.promfg.2020.08.143>
17. Zhang H, Qin S, Cao L (2021) Investigation of the effect of blank holder force distribution on deep drawing using developed blank holder divided into double rings. *J Brazilian Soc Mech Sci Eng.* <https://doi.org/10.1007/s40430-021-03003-7>
 18. Salahshoor M, Gorji H, Bakhshi-Jooybari M (2019) Analysis of the effects of tool and process parameters in hydrodynamic deep drawing assisted by radial pressure. *J Brazilian Soc Mech Sci Eng.* <https://doi.org/10.1007/s40430-019-1648-4>
 19. Butuc MC, Gracio JJ, Barata da Rocha A (2003) A theoretical study on forming limit diagrams prediction. *J Mater Process Technol* 142(3):714–724. [https://doi.org/10.1016/S0924-0136\(03\)00813-6](https://doi.org/10.1016/S0924-0136(03)00813-6)
 20. Hill R (1948) A theory of the yielding and plastic flow of anisotropic metals. *Proc R Soc A Math Phys Eng Sci* 193(1033):281–297
 21. Hill R (1952) On discontinuous plastic states, with special reference to localized necking in thin sheets. *J Mech Phys Solids* 1(1):19–30. [https://doi.org/10.1016/0022-5096\(52\)90003-3](https://doi.org/10.1016/0022-5096(52)90003-3)
 22. Banabic D, Barlat F, Cazacu O, Kuwabara T (2020) Advances in anisotropy of plastic behaviour and formability of sheet metals. *Int J Mater Form* 13(5):749–787. <https://doi.org/10.1007/s12289-020-01580-x>
 23. Hou Y, Min J, Lin J, Liu Z, Carsley JE, Stoughton TB (2017) Springback prediction of sheet metals using improved material models. *Proced Eng* 207:173–178. <https://doi.org/10.1016/j.pro-eng.2017.10.757>
 24. Barlat F, Lian K (1989) Plastic behavior and stretchability of sheet metals. Part I: a yield function for orthotropic sheets under plane stress conditions. *Int J Plast* 5(1):51–66. [https://doi.org/10.1016/0749-6419\(89\)90019-3](https://doi.org/10.1016/0749-6419(89)90019-3)
 25. Barlat F et al (2003) Plane stress yield function for aluminum alloy sheets - part 1: theory. *Int J Plast* 19(9):1297–1319. [https://doi.org/10.1016/S0749-6419\(02\)00019-0](https://doi.org/10.1016/S0749-6419(02)00019-0)
 26. Chen G, Zhao C, Shi H et al (2022) Nonlinear kinematic hardening constitutive model based on Hill48 yield criterion and its application in reverse deep drawing. *J Braz Soc Mech Sci Eng* 44:471. <https://doi.org/10.1007/s40430-022-03741-2>
 27. Padmanabhan R, Oliveira MC, Alves JL, Menezes LF (2007) Influence of process parameters on the deep drawing of stainless steel. *Finite Elem Anal Des* 43(14):1062–1067. <https://doi.org/10.1016/j.finel.2007.06.011>
 28. Raju S, Ganesan G, Karthikeyan R (2010) Influence of variables in deep drawing of AA 6061 sheet. *Trans Nonferrous Met Soc China* 20(10):1856–1862. [https://doi.org/10.1016/S1003-6326\(09\)60386-1](https://doi.org/10.1016/S1003-6326(09)60386-1)
 29. Luyen T-T, Pham Q-T, Mac T-B, Banh T-L, Nguyen D-T (2021) Graphical method based on modified maximum force criterion to indicate forming limit curves of 22MnB5 boron steel sheets at elevated temperatures. *J Iron Steel Res Int* 28(8):1009–1018. <https://doi.org/10.1007/s42243-021-00567-5>
 30. BK and Hibbit PSD (2001) ABAQUS/CAE User's Manual. Ver. 6.10.1. ABAQUS Inc, pp 1–847
 31. Sheng ZQ, Jiratheeranat S, Altan T (2004) Adaptive FEM simulation for prediction of variable blank holder force in conical cup drawing. *Int J Mach Tools Manuf* 44(5):487–494. <https://doi.org/10.1016/j.ijmactools.2003.11.001>
 32. Basril MAM et al (2017) The effect of heating temperature and methods towards the formability of deep drawn square metal cup. *IOP Conf Ser Mater Sci Eng* 210:012067

Publisher's Note Springer Nature remains neutral with regard to jurisdictional claims in published maps and institutional affiliations.

Springer Nature or its licensor (e.g. a society or other partner) holds exclusive rights to this article under a publishing agreement with the author(s) or other rightsholder(s); author self-archiving of the accepted manuscript version of this article is solely governed by the terms of such publishing agreement and applicable law.